ARTICLES

Rheology and Structures of Aqueous Gels of Diblock(Oxyethylene/Oxybutylene) Copolymer $E_{22}B_7$

Withawat Mingvanish,[†] Antonis Kelarakis,[‡] Shao-Min Mai,[†] Christophe Daniel,[§] Zhuo Yang,[†] Vasiliki Havredaki,[‡] Ian W. Hamley,[§] Anthony J. Ryan,[||] and Colin Booth*,[†]

Department of Chemistry, University of Manchester, Manchester M13 9PL, U.K., National and Kapodistrian University of Athens, Department of Chemistry, Physical Chemistry Laboratory, Panepistimiopolis, 157 71 Athens, Greece, School of Chemistry, University of Leeds, Leeds LS2 9JT, U.K., and Department of Chemistry, University of Sheffield, Sheffield S3 7HF, U.K.

Received: April 13, 2000; In Final Form: August 11, 2000

The phase behavior of an oxyethylene/oxybutylene diblock copolymer ($E_{22}B_7$) in aqueous solution was defined using three properties: yield stress (by rheometry and tube inversion), dynamic modulus (by rheometry), and structure (by small-angle X-ray scattering). The boundary of immobile, structured gel (hard gel) was detected by all three methods, giving satisfactory agreement. A structural transition within the hard gel, from bcc to hex, was detected by rheometry and SAXS. Two types of soft gel were detected and assigned to disordered phases containing either spherical or cylindrical micelles. Comparison with results for other diblock E_mB_n copolymers showed a regularity of behavior influenced largely by oxyethylene-block length, with oxybutylene-block length having a minor but significant role.

1. Introduction

Block copolymers of poly(oxyethylene) and poly(oxybutylene) in dilute aqueous solutions form micelles, and more concentrated micellar solutions form liquid-crystal mesophases (gels). A number of studies of diblock E_mB_n aqueous gels have been reported: see ref 1 for publications prior to 1999; references 2−5 thereafter. In present notation E denotes oxyethylene, OCH_2CH_2, and B denotes oxybutylene, $OCH_2CH(C_2H_5)$, while the subscripts denote number-average block lengths in repeat units. Recent work on the rheology and structures (by small-angle X-ray scattering, SAXS) of cubic phases of packed spherical micelles has been summarized,[3] attention being primarily focused on copolymers with E blocks of 100 repeat units or more: for example the series $E_{96}B_{18}$, $E_{184}B_{18}$, $E_{315}B_{17}$, and $E_{398}B_{19}$.[2−4] The work described in this paper stems from an interest in the cubic-to-hexagonal (hex) transition in aqueous solutions of diblock E_mB_n copolymers with much shorter E blocks.

Cubic and hex phases have been defined by rheometry and polarized light microscopy for aqueous solutions of copolymer $E_{41}B_8$,[6] and the following structures confirmed by small-angle X-ray scattering (SAXS): cubic (bcc) for a 40 wt % solution; hex for a 60 wt % solution,[7] indicating a cubic/hex transition at or about 50 wt % copolymer. No thermally induced cubic/hex transition was observed in these experiments. Aqueous gels of copolymer $E_{18}B_{10}$, which is available commercially from The Dow Chemical Company,[8] have been studied by Alexandridis et al.,[9] who recorded SAXS from samples held at 25 °C. They reported that the 23 wt % gel was bcc and the 42 wt % gel was hex. Recently Fairclough et al.[10] have used SAXS in a preliminary study of solutions of $E_{18}B_{10}$ at selected temperatures. A 40 wt % solution was found to be a cubic gel at 13 °C but a hex gel at 40 °C, while a 50 wt % solution was a hex gel at 20 °C.

A transition from cubic to hex gel at high concentrations is a well-documented effect forced by packing considerations, i.e., by exceeding the limiting value of the effective volume fraction ($\phi = 0.68-0.74$) placed on cubic packing (bcc or fcc) of water-swollen micelles acting as hard spheres, compared with a limiting value of $\phi = 0.91$ for cylindrical micelles in a hexagonal array. Thermally induced transitions are less well documented, certainly so for aqueous gels of poly(oxyalkylene) diblock copolymers, where that for the 40 wt % solution of $E_{18}B_{10}$ is the only example. In this paper we describe a study of aqueous gels of block copolymer $E_{22}B_7$ in water. Following Hoffmann and co-workers,[11] the ratio of E-block length to hydrophobic-block length (*m/n*) can be used as an indicator of the likelihood of hex gel formation. The lower the value of *m/n*, the more likely is the hex phase. For the three copolymers discussed above, the values of *m/n* are

copolymer	$E_{41}B_8$	$E_{22}B_7$	$E_{18}B_{10}$
m/n	5.1	3.3	1.8

which places $E_{22}B_7$ between the two copolymers previously studied.

2. Experimental Section

The preparation of copolymer $E_{22}B_7$ was by sequential anionic polymerization of ethylene oxide followed by 1,2-butylene

[†] University of Manchester.
[‡] National and Kapodistrian University of Athens.
[§] University of Leeds.
[||] University of Sheffield.

10.1021/jp001398o CCC: $19.00
Published on Web 10/03/2000

TABLE 1: Molecular Characteristics of Block Copolymer $E_{22}B_7$[a]

wt % E(NMR)	M_n/g mol^{-1} (NMR)	M_w/M_n (GPC)
65.7	1470	1.03

[a] Estimated uncertainties: ±3% in M_n and block lengths: ±0.01 in M_w/M_n.

oxide, as described previously for other E_mB_n copolymers.[12] Gel permeation chromatography (GPC) was used to confirm a narrow chain length distribution, and ^{13}C NMR spectroscopy was used to obtain an absolute value of the number-average molar mass and to confirm the diblock architecture. The molecular characteristics of the copolymer are summarized in Table 1.

To prepare a solution, copolymer and water were weighed into a vessel and mixed in the mobile state (at an appropriate temperature, see section 3.1) before being stored for several days at refrigerator temperature ($T \approx 5$ °C). Newly prepared samples were used for each experiment.

Rheological properties of the samples were determined using a Bohlin CS50 rheometer with water-bath temperature control. Couette geometry (bob, 24.5 mm diameter, 27 mm height; cup, 26.5 mm diameter, 29 mm height) was used for all the samples, with 2.5 cm^3 of sample being added to the cup. A solvent trap maintained a water-saturated atmosphere around the cell. Storage and loss moduli were recorded across the temperature range with the instrument in oscillatory-shear mode at a frequency of 1 Hz and at low strain amplitude (<0.5%, linear viscoelastic region). Samples were heated at 1 °C min^{-1} in the range 5−95 °C. Measurements of yield stress were made at selected temperatures with the instrument in steady-shear mode and programmed to increase the shear stress in a series of logarithmically spaced steps, allowing 1 min between each step. Usually a period of 20 min was allowed for temperature equilibration before starting the program at any given temperature. We are aware that the properties of low-modulus gels (particularly soft gels) are strongly dependent on frequency.[4,13] However, the amount of sample available precluded investigation of this effect, and a fixed frequency of 1 Hz was used throughout the work.

In related experiments, samples (0.5 g) were enclosed in small tubes (internal diameter ca. 10 mm) and observed while slowly heating (or cooling) the tube in a water bath within the range 0−85 °C. The heating/cooling rate was 0.5 °C min^{-1}. The change from a mobile to an immobile system (or vice-versa) was determined by inverting the tube. At the same time, any clouding (i.e., phase separation) was detected by eye.

SAXS experiments were conducted at the Synchrotron Radiation Source, Daresbury Laboratory, U.K. Samples of concentration 30 and 35 wt % were subjected to shear using a Couette cell described elsewhere.[14] The X-ray beam was in the radial direction, i.e., it passed through the center of the Couette cell. A water bath enabled investigation of samples under a controlled heating ramp. Samples in the concentration range 40−80 wt % were enclosed in modified DSC cells and heated (5 °C min^{-1}) in a Linkam DSC instrument. This instrumentation has been described elsewhere.[15]

3. Results and Discussion

3.1 Tube Inversion. Results from tube inversion tests are set out in Figure 1. Mobile, immobile, and turbid regions were well defined in the concentration range 1−85 wt % copolymer, as indicated in the figure. The gap at $c = 45$ wt %, $T = 37-45$ °C indicates a clear-mobile interval in the boundary which is associated with the cubic-hex transition, evidence for which is described in subsequent sections. A turbid gel, detected at high concentrations and low temperatures, is ascribed to crystallization: the melting point of the pure copolymer is $T_m \approx 37$ °C. The boundary of the immobile-gel region is similar to those reported for other E/B copolymers with various block architectures: for example $E_{38}B_{12}$, $E_{21}B_{11}E_{21}$, and $B_7E_{40}B_7$,[16] and also bears some resemblance to those reported for C/E cooligomers which show a cubic phase followed by a hex phase as concentration is increased: for example $C_{12}E_8$ and $C_{16}E_{12}$.[17]

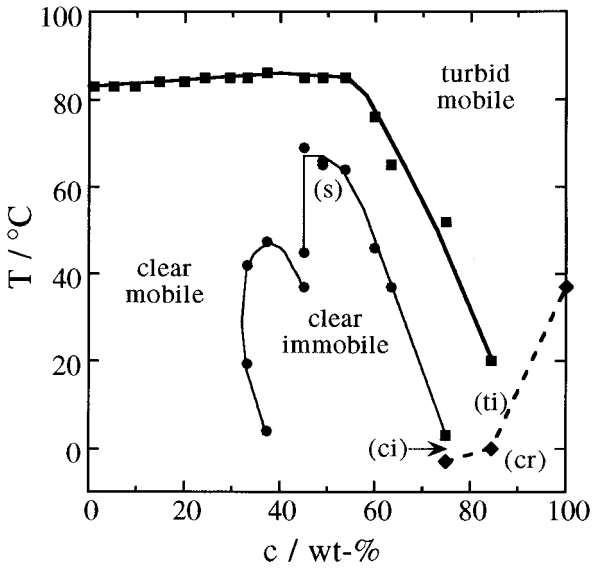

Figure 1. Mobile-immobile and clouding boundaries detected by tube-inversion for solutions of copolymer $E_{22}B_7$. There is a "clear mobile" interval in the boundary at $c = 45$ wt %, $T = 37-45$ °C. (s) indicates separation of a small amount of water from the immobile gel (syneresis) at temperatures exceeding 58 °C. Boundaries at low temperatures were not defined: (ci) and (ti) indicate observation of clear-immobile and turbid-immobile phases; (cr) indicates a very-turbid (white) phase associated with crystallization.

3.2 Rheometry. In describing complex systems of this type, Hvidt et al.[18] have used yield stress (σ_y) and modulus (storage and loss, G' and G'') to define three convenient subdivisions of the range of behaviors observed: immobile "hard gel" (high σ_y and G', $G' > G''$), mobile "soft gel" (low σ_y and G', $G' > G''$), and mobile sol (zero σ_y and very low G', $G'' > G'$). We adopt this notation here.

3.2.1 Storage and Loss Modulus. The temperature dependences of the storage and loss moduli of aqueous solutions of copolymer $E_{22}B_7$ (determined using oscillatory shear at $f = 1$ Hz) are shown in Figure 2. The concentration range (35−60 wt % copolymer) covers the region of clear immobile gels: see Figure 1. A general feature is very low values of the moduli at temperatures exceeding 65 °C, where all the systems are sols ($G'' > G'$). The temperatures at which values of G' fall sharply coincide well with the immobile/mobile boundary illustrated in Figure 1: details are given in Table 2, where the 37 °C point for the 45 wt % solution is for the low-T transition seen in Figure 2. The high-modulus gels (10^4 Pa or more) formed at low temperatures and concentration 35−45 wt % are assigned to cubic-packed spherical-micelle structures, while the moderate-modulus gels (ca. 10^3 Pa) at higher concentrations are assigned to hexagonally packed cylindrical-micelle structures. These structures are listed in Table 2 and confirmation of the structures by SAXS is described in section 3.3. The cubic and hex gels are immobile in the tube inversion test and can be classified as hard gels.

The moduli of the high-concentration solutions ($c \geq 45$ wt %) fell continuously within the temperature range examined,

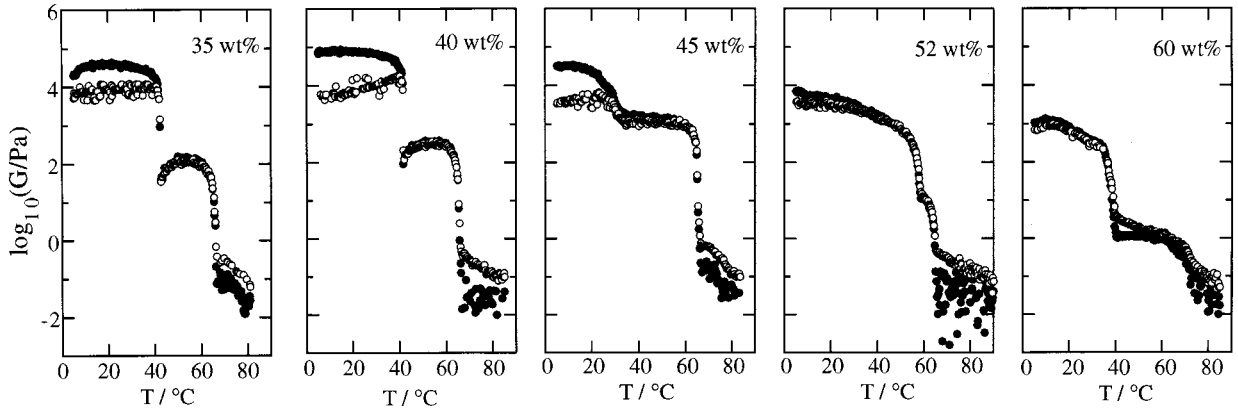

Figure 2. Temperature dependences of logarithmic storage and loss moduli ($f = 1$ Hz) for aqueous solutions of copolymer $E_{22}B_7$. Filled symbols denote log(G') and unfilled symbols denote log(G''). Copolymer concentrations (wt %) are indicated.

TABLE 2: Upper Boundary (T °C) of Hard Aqueous Gels of Copolymer $E_{22}B_7$

c/wt %	tube inversion	rheometry	SAXS
35	44	43 (cubic)	37 (bcc)
40	46	42 (cubic)	44 (bcc)
45	37	35 (cubic)	
65	60 (hex)		
47	67		71 (hex)
37 (bcc)			
52	64	65 (hex)	76 (hex)
27 (bcc)			
60	45	40 (hex)	47 (hex)

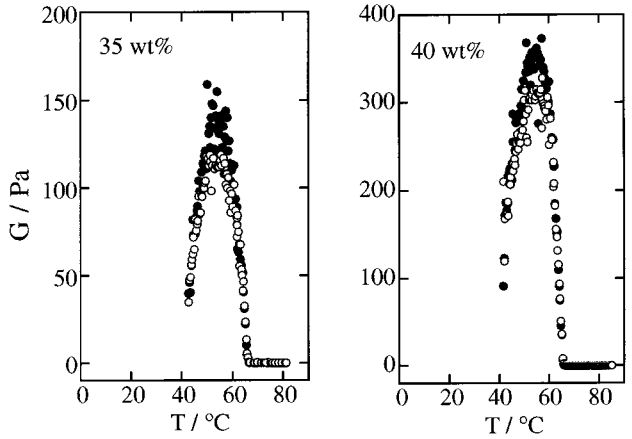

Figure 3. Temperature dependences of storage and loss moduli ($f =$ 1 Hz) for soft aqueous gels of copolymer $E_{22}B_7$. Filled symbols denote G' and unfilled symbols denote G''. Copolymer concentrations (wt %) are indicated.

whereas those of the 35 and 40% gels passed through a discontinuity at $T = 42-43$ °C. The data obtained for the 45 wt % solution showed no evidence of the clear-mobile interval seen in the tube-inversion test, possibly because the concentration (known to ±0.1 wt %) is marginally higher. The data at temperatures above the discontinuity are replotted on a linear scale in Figure 3. For the 40 wt % sample, starting at $T \approx 42$ °C the value of G' rose to 360 Pa before falling sharply to a very low value at $T \approx 65$ °C. The corresponding plot for the 35 wt % sample had a lower maximum value of $G' \approx 150$ Pa. As can be seen in Figure 3, near the maximum G' exceeds G'' and consequently this mobile fluid can be categorized as a soft gel. For convenience in subsequent discussion, this type of soft gel is denoted A.

Temperature scans were also carried out for solutions at concentrations below the hard-gel limit (i.e., at 30, 26, and 22.5 wt %). A soft gel region was detected in the temperature range 25−45 °C and concentration range 22.5−35 wt %, as indicated by the temperature-modulus curves for the 22.5 and 30 wt % samples shown in Figure 4. The maximum modulus found for the 26 wt % sample was $G' \approx 170$ Pa compared with 340 Pa for the 30 wt % sample, and only 8 Pa for the 22.5 wt % sample. No indication of soft gel was found for a 20 wt % solution. The soft gels in this temperature range are denoted B.

In Figure 4, weak features in the $G(T)$ curves of the 26 and 30 wt % samples can be seen in the approximate temperature range 45−65 °C. The maxima are $G' < 10$ Pa. Expansion of the ordinate (not shown, but see the curves for the 22.5 wt % solution) revealed that G' exceeded G'' which, together with the temperature range of 45−65 °C, allows these features to be assigned to soft-gel A.

The relationship between the hard and soft gels is illustrated in Figure 5, where the hard gel boundary from the tube-inversion experiments (Figure 1) is reproduced, and the data points defining the soft gel boundaries from rheology are added. Data points obtained by rheology for the boundary of the hard gel regions are included. The correspondence between hard gel boundaries obtained by the two methods has been remarked upon above (see Table 2). The position of soft-gel A on the temperature scale coincides with that of the hex hard gels (see, for example, Figure 2, 45 wt % gel), indicating that the soft gel in this region may well contain cylindrical micelles. Soft gels containing cylindrical micelles have been described for aqueous solutions of triblock oxyethylene/oxypropylene copolymers [$E_mP_nE_m$, where P denotes $OCH_2CH(CH_3)$],[18,19] and micellar sphere-to-rod transitions have been confirmed in dilute aqueous solution for a number of copolymers, particularly $E_{27}P_{39}E_{27}$ (coded P85)[19,20] but also including diblock copolymer $E_{18}B_{10}$.[21] The temperature range of soft-gel B is that assigned to cubic gels, i.e., packed spherical micelles. This type of soft-gel behavior has been attributed to a percolation mechanism whereby structures of weakly interacting spherical micelles form in the system.[4,6,22] The transition from sol to soft gel is assumed to occur when micellar aggregates reach a percolation threshold yielding sufficient structure to cause an increase in modulus and, at a suitable frequency, the dynamic storage modulus to exceed the loss modulus.

3.2.2 Yield Stress. The response of the cubic hard gels to increase in stress was fracture at a high value, $\sigma_y \approx 1$ kPa or more. The high-T hard gels of the lower modulus hex gels yielded at significantly lower stress ($\sigma_y = 100-200$ Pa) to give a shear-thinning fluid. The high-temperature sols had zero yield stress and Newtonian viscosity. Examples of these behaviors

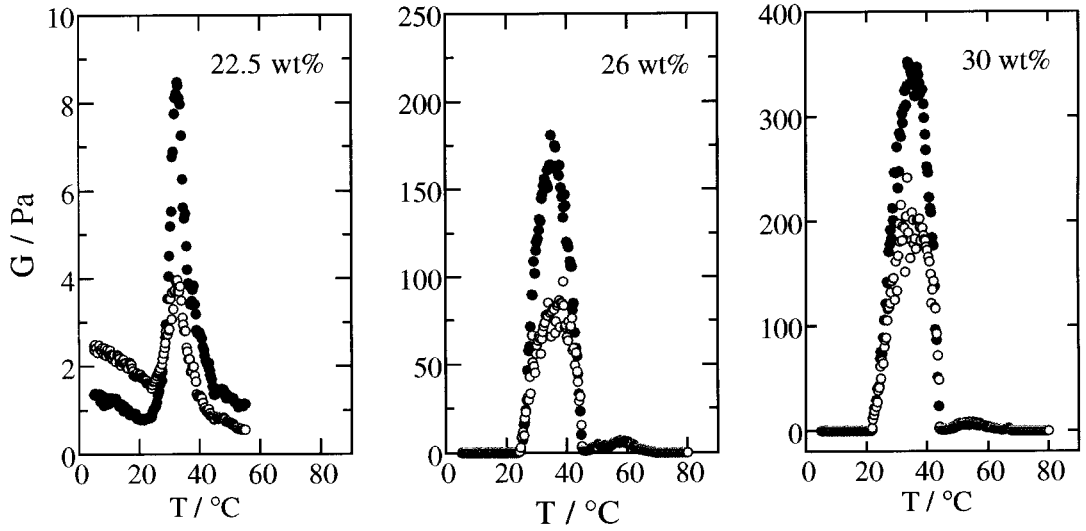

Figure 4. Temperature dependences of storage and loss moduli ($f = 1$ Hz) for soft aqueous gels of copolymer $E_{22}B_7$ at concentrations below the limiting value for hard gel formation. Filled symbols denote G' and unfilled symbols denote G''. Copolymer concentrations (wt %) are indicated.

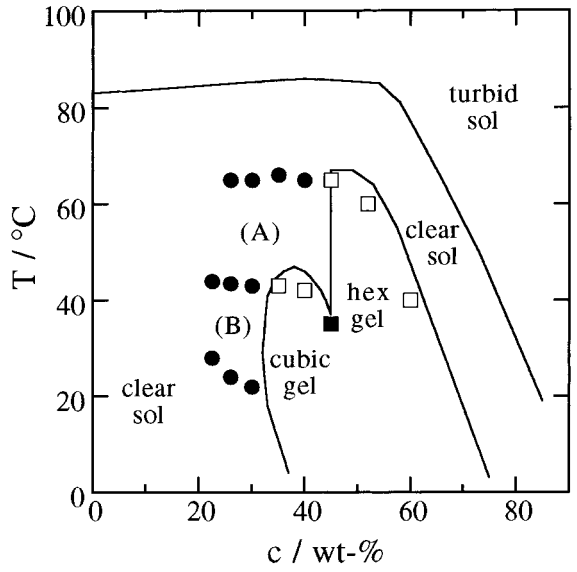

Figure 5. Phase boundaries and results from rheometry. The lines show mobile-immobile and clouding boundaries taken from Figure 1. The points denote (●) soft-gel boundaries, (□) hard-gel boundaries, and (■) a cubic/hex transition. The assignment to cubic and hexagonal hard gels is on the basis of storage modulus (see text). The soft gels are attributed to disordered phases containing (A) cylindrical micelles and (B) spherical micelles.

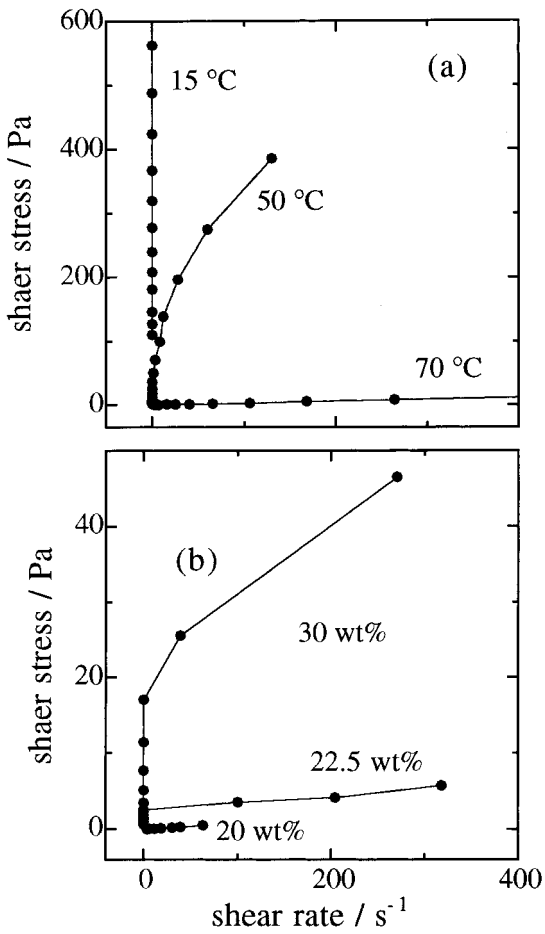

Figure 6. Shear stress versus shear rate for aqueous solutions of copolymer $E_{22}B_7$ under steady shear. (a) Hard gels (45 wt %) at the temperatures indicated. The cubic gel at 15 °C finally yielded at 1500 Pa. At 70 °C the system was a sol. (b) Soft gels at 35 °C and the concentrations indicated. At 20 wt % the system was a sol.

are shown for the 45 wt % gel in Figure 6a, and selected values of the yield stress are listed in Table 3. Values of σ_y/G' (the latter read off plots such as those shown in Figure 2) averaged 0.03 ± 0.01 for the bcc gels, similar to that reported previously for fcc gels of E_mB_n copolymers,[4] and 0.10 ± 0.03 for the hex gels.

As expected the soft gels had very low yield stresses: see Figure 6b and Table 3. Clearly these yield stresses, $\sigma_y \leq 20$ Pa, were insufficient to stop flow in the tube-inversion test.

3.3 Gel Structure from SAXS. The results of the SAXS experiments are summarized in Table 4, and the transitions defined by the experiments are mapped onto the "tube-inversion" boundary in Figure 7, as discussed below.

Couette rheometry was used in experiments 1 and 2 (30 and 35 wt % solutions). The SAXS patterns obtained were essentially those of unoriented phases irrespective of applied shear at rates up to 100 s^{-1} (steady) and 50 s^{-1} with 100% strain amplitude (oscilliatory). Accordingly, it is convenient to represent the 2-dimensional SAXS pattern by a one-dimensional plot of intensity against q/q^*, where $q = (4\pi/\lambda)\sin(\theta/2)$ is the scattering vector, λ is the wavelength (1.5 Å), θ is the scattering

TABLE 3: Typical Yield Stresses of Aqueous Gels of Copolymer $E_{22}B_7$

c/wt %	*T*/°C	structure	σ_y/Pa
hard gel			
35	25	cubic	600
40	25	cubic	1500
45	15	cubic[a]	1500
45	50	hex[a]	100
60	15	hex	180
soft gel A			
40	45		8
soft gel B			
22.5	35		3
30	35		20

[a] Based on $G'(T)$ − see Figure 2.

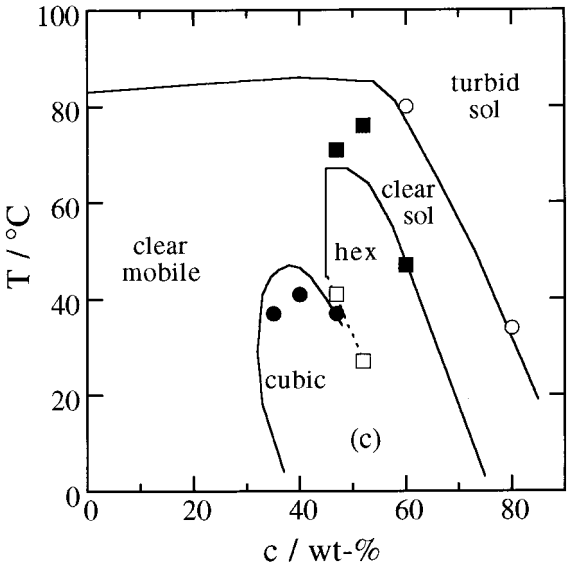

Figure 7. Phase boundaries and results from SAXS. The full lines show mobile−immobile and clouding boundaries taken from Figure 1 extended to show part of the upper boundary of the bcc phase. The dotted line indicates part of the lower boundary of the hex phase, and (c) indicates a region in which the SAXS pattern is complex. The data points indicate the limits of characteristic scattering patterns: i.e., the high-*T* limits of the (●) bcc, (■) hex and (○) micellar patterns, and the low-*T* limit of the (□) hex pattern. Note that the hex pattern extends into the mobile region, and its disappearance may relate to flow of the sample away from the X-ray beam. See Figure 5 for soft-gel regions.

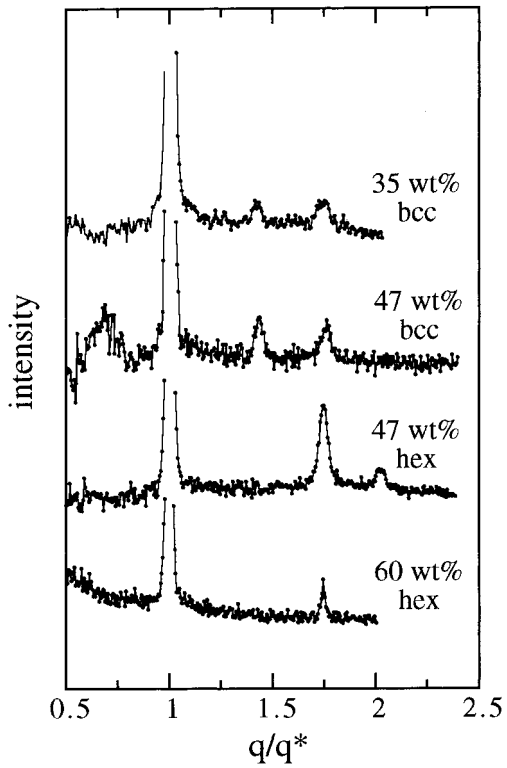

Figure 8. Examples of SAXS patterns for aqueous solutions of block copolymer $E_{22}B_7$. From top to bottom (as indicated): 35 wt % gel at 20 °C, bcc, $q^* = 0.0807$ Å^{-1}; 47 wt % gel at 10−30 °C, bcc, $q^* = 0.0809$ Å^{-1}; 47 wt % gel at 55−70 °C, hex, $q^* = 0.0856$ Å^{-1}; 60 wt % gel at 10−40 °C, hex, $q^* = 0.0938$ Å^{-1}. The patterns are averaged over the temperature ranges specified.

angle, and q^* is the value of q at the first-order maximum. A pattern from the 35 wt % hard gel at 20 °C is shown in Figure 8: the peaks at $q/q^* = 1, \sqrt{2}, \sqrt{3}$ are characteristic of a bcc structure. At temperatures higher than 37 °C, the SAXS pattern was a broad ring characteristic of a micellar solution, irrespective of whether the phase was a soft gel or a sol. The SAXS patterns of the 30 wt % solution, i.e., below the limiting concentration for hard-gel formation, showed a broad ring across the whole *T*-range investigated.

The samples in the DSC experiments were held under quiescent conditions, and SAXS patterns were plotted at intervals as the samples were heated at 5 °C min^{-1}. In this procedure, because the pans were mounted vertically in the instrument, scattering after the sample entered its mobile phase could not be consistently measured for the more dilute samples (40−52 wt %), as they could flow out of the beam. More consistent measurements were possible for concentrated samples (60−80 wt %).

The scattering patterns obtained for the 40 wt % sample (not illustrated) indicated a bcc phase below 41 °C and a micellar fluid (broad peak) for a few °C thereafter. Figure 9a shows successive plots obtained for the 47 wt % gel: the pattern corresponds to a bcc phase from 10 to 37 °C, to a transition from 37 to 41 °C, and to a hex phase ($q/q^* = 1, \sqrt{3}, \sqrt{4}$) from 41 to 71 °C. Patterns obtained by averaging over a limited temperature range are illustrated in Figure 8. Persistence of a hex scattering pattern to temperatures beyond that of the mobile/immobile transition, which is noted in Table 2 and illustrated in Figure 7, has been remarked upon before in connection with hex gels of copolymer $E_{41}B_8$.[7] In those experiments the gels were contained in tubes, and the effect could be followed over a wider temperature range.[7]

The scattering patterns (not illustrated) obtained for the 52 wt % gel at temperatures above 24 °C were from a hex structure. Again the hex pattern was detected some degrees above the hard-gel boundary, i.e., until the sample flowed out of the beam (see Figure 7). The scattering patterns from this sample at low temperatures (<24 °C) contained both sharp peaks and broad peaks, and could not be assigned to a single structure. No transition was detected at 24 °C in the $G'(T)$ curve of this gel (see Figure 2).

Figure 9b shows scattering from the 60 wt % gel as temperature was changed from 10 to 90 °C. The pattern is that expected for a hex gel: see also Figure 8. On heating into the mobile phase at higher temperatures the sharp peaks were replaced by a single broad peak. The temperature at which the broad peak in the SAXS patterns could no longer be detected (80 °C) coincided with the cloud-point curve: see Figure 7. A similar broad peak (but no sharp peaks) was observed in the SAXS pattern of the 80 wt % sample at $T < 34$ °C. At this high concentration and low temperatures, crystallization of the

TABLE 4: Structural Information from SAXS for Aqueous Solutions of Copolymer $E_{22}B_7$

expt		c/wt %	T-range/°C	result
1	Couette	30	20−75	broad ring
2	Couette	35	5−60	5 → bcc → 37 → broad ring
3	DSC	40	10−50	10 → bcc → 44 → broad peak
4	DSC	47	10−75	10 → bcc → 37−41 → hex → 71
5	DSC	52	0−75	0 → (*a*) → 27 → hex → 76
6	DSC	60	10−90	10 → hex → 47 → broad peak → 80 → no peak detected
7	DSC	80	10−90	10 → broad peak → 34 → very broad peak

[a] Complex SAXS pattern: no structure assigned.

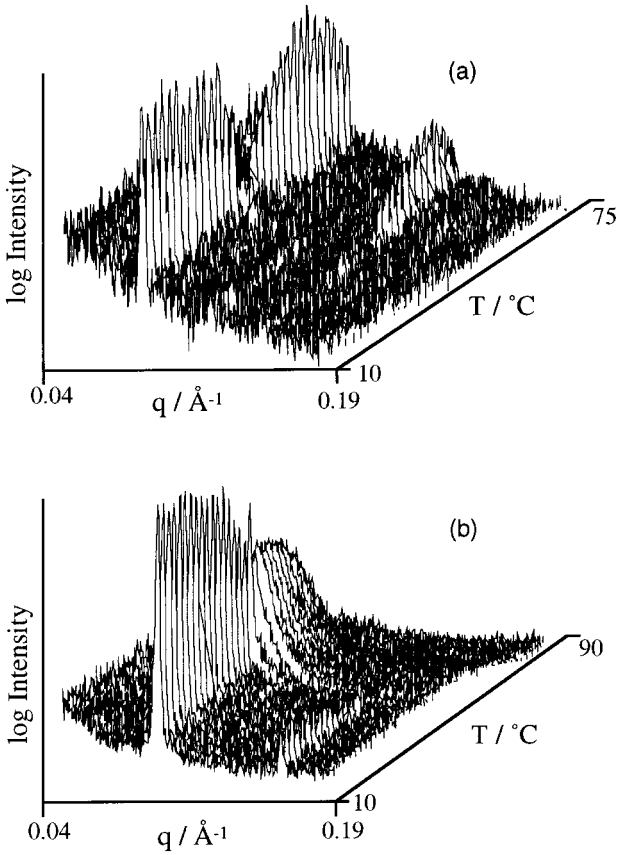

Figure 9. Log(scattering intensity) versus scattering vector versus temperature for aqueous solutions of block copolymer $E_{22}B_7$: (a) 47 wt %; (b) 60 wt %.

E-block was a possibility. Accordingly, wide-angle X-ray scattering (WAXS) recorded simultaneously with the SAXS,[14,15] was used to confirm the noncrystalline nature of the sample. As for the 60 wt % sample, the temperature at which the broad peak was no longer detectable coincided with the clouding temperature.

Turning to the detail of Figure 7 and considering first the concentration range 45−52 wt %, the lower boundary of the hex phase (shown by the dotted line) is separated from the upper boundary of the bcc phase by a narrow region of undefined structure, assumed to be biphasic bcc/hex. Because the 60 wt % solution gave a hex scattering pattern down to 10 °C, it is certain that the lower boundary of the hex gel passes through that temperature somewhere in the interval 52−60 wt %. Similarly, because the 47 wt % solution gave a bcc scattering pattern down to 10 °C, it can be concluded that the upper boundary of the bcc phase reaches 10 °C somewhere in the interval 47−52 °C. These conclusions are supported by the results from rheology. It was not possible to define these low-temperature boundaries more closely. In the same concentration range (45−52 wt %) the upper boundary of the immobile gel

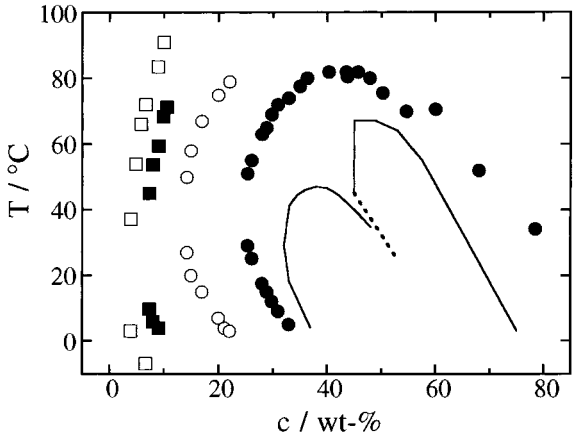

Figure 10. Hard-gel boundaries for aqueous solutions of E_mB_n diblock copolymers. The curves show the present data for $E_{22}B_7$. Other results are for: (●) $E_{41}B_8$; (○) $E_{90}B_{10}$; (■) $E_{210}B_{16}$; (□) $E_{398}B_{19}$.

(solid line in Figure 7, confirmed by rheology as shown in Figure 5), is characterized by a transition to a sol showing hex structure, i.e., a sol with the characteristics of a nematic phase. Considering the 35 and 40 wt % solutions, the bcc scattering patterns from SAXS disappear a few degrees lower than the immobile/mobile boundary from the tube inversion test (and similarly below the boundary defined by rheology, see Figure 5). In this region the immobile/mobile transition is to soft gel A, assumed to contain cylindrical micelles. It may be that the hard bcc gel changes on heating to an intermediate hard gel containing both spherical and cylindrical micelles before completing the transition to the soft gel.

4. Comparison with Previous Work on Diblock E_mB_n Diblock Copolymers

Figure 10 provides an impression of the overall pattern of hard-gel boundaries defined for aqueous E_mB_n diblock copolymer gels in this and previous work.[2,6,23] The results selected are for copolymers $E_{22}B_7$, $E_{41}B_8$, $E_{90}B_{10}$, $E_{210}B_{16}$, and $E_{394}B_{19}$: for the last three copolymers data are available only for low concentrations. Similar results are not available for copolymer $E_{18}B_{10}$. The gels first formed on increasing the copolymer concentration are body-centered cubic in structure,[1,3,4,7,23,24] and presumed to comprise packed spherical micelles. The exception is copolymer $E_{41}B_8$ for which SAXS indicates a narrow band of face-centered cubic gel before the bcc structure is established.[7] Ignoring details, it is clear from Figure 10 that the variation in gelation behavior near to the limiting concentration for gelation (c^*) is of degree and not of kind. The major effect is that of E-block length: c^* decreases from 32 wt % to 3.5 wt % along the series from E_{22} to E_{398}. The effect of the increase in B-block length along the series is to render the micelles more stable at low temperatures (i.e., where water is a better solvent for the E blocks) and thereby to stabilize the gel in that region. Both of these effects have been discussed recently.[1,2,4]

TABLE 5: Storage Modulus Measured at 20 °C and 1 Hz for Aqueous Gels of E_mB_n Copolymers with bcc Structure

copolymer	c/wt %	(c-c^*)/wt %	G'/kPa
$E_{22}B_7$	35−40	3−7	30−80
$E_{41}B_8$	30	5	40
$E_{184}B_{18}$	10	5.5	7
$E_{398}B_{19}$	8.5	5	8

Of the five copolymers included in Figure 10, only $E_{22}B_7$ and $E_{41}B_8$ have been shown to form hexagonal gels. Indications are that gels formed from copolymers with long E blocks remain bcc up to high concentrations, e.g., 70 wt % in the case of copolymer $E_{90}B_{10}$. The complex phase diagram of copolymer $E_{22}B_7$ results from the cubic/hex thermal transition, an effect which has not been found for the $E_{41}B_8$ system. The results of Fairclough et al. for aqueous solutions of $E_{18}B_{10}$, described in the Introduction to this paper, indicate similar gelation behavior to that of $E_{22}B_7$.

Considering the storage modulus from oscillatory-shear measurements it is possible to compare values within the bcc region and at similar (c-c^*), taking due account of temperature and frequency. Values of G' for bcc gels of concentration (c-c^*) $\approx$ 5 wt % are available for three of the copolymers considered above: $E_{22}B_7$, $E_{41}B_8$, and $E_{398}B_{19}$ and related data for copolymer $E_{184}B_{18}$ may be added: see Table 5. The values of G' listed fall into two groups, and relate to concentration rather than to copolymer composition. Unfortunately, values of G' at constant concentration are not available for the series.

Soft gel regions have been defined[4,6] for aqueous solutions of diblock copolymers $E_{22}B_7$, $E_{41}B_8$, and the series of four based on B_{17-19} of which results for $E_{398}B_{19}$ and $E_{184}B_{18}$ have been considered above.[4,6] Of these, only the soft gels of $E_{22}B_7$ show a cubic → hex transition on heating. As discussed above, this transition parallels the bcc → hex transition of the hard gel and can be assigned to a change from spherical to cylindical micelles.

Acknowledgment. W.M. was supported by the Thai Government, and C.D. by the EU-TRM network "Complex Architectures in Diblock Based Copolymer Systems". Support for polymer synthesis and SAXS at the Daresbury facility was through EPSRC grants GR/L22645 and GR/L79854. Dr. J. P. A. Fairclough kindly provided an account of work on $E_{18}B_{10}$ aqueous gels carried out at Sheffield University (ref 10).

References and Notes

(1) Derici, L.; Ledger, S.; Mai, S.-M.; Booth, C.; Hamley, I. W.; Pedersen, J. S. *Phys. Chem. Chem. Phys.* **1999**, *1*, 2773.

(2) Mingvanish, W.; Mai, S.-M.; Heatley, F.; Booth, C.; Attwood, D. *J. Phys. Chem. B* **1999**, *103*, 11269.

(3) Hamley, I. W.; Daniel, C.; Mingvanish, W.; Mai, S.-M.; Booth, C.; Messe, L.; Ryan, A. J. *Langmuir* **2000**, *16*, 2508.

(4) Kelarakis, A.; Mingvanish, W.; Daniel, C.; Li, H.; Havredaki, V.; Booth, C.; Hamley, I. W., Ryan, A. J. *Phys. Chem. Chem. Phys.* **2000**, *2*, 2755.

(5) Daniel, C.; Hamley, I. W.; Mingvanish, W.; Booth, C. *Macromolecules* **2000**, *33*, 2163.

(6) Li, H.; Yu, G.-E.; Price, C.; Booth, C.; Hecht, E.; Hoffmann, H. *Macromolecules* **1997**, *30*, 1347.

(7) Fairclough, J. P. A.; Ryan, A. J.; Hamley, I. W.; Li, H.; Yu, G.-E.; Booth, C. *Macromolecules* **1999**, *32*, 2058.

(8) Nace, V. M. *J. Am. Oil. Chem. Soc.* **1996**, *73*, 1: Yu, G.-E.; Yang, Y.-W.; Yang, Z.; Attwood, D.; Booth, C.; Nace, V. M. *Langmuir* **1996**, *12*, 3404.

(9) Alexandridis, P.; Olsson, U.; Lindman, B. *Langmuir* **1997**, *13*, 23.

(10) Fairclough, J. P. A.; Weston, M.; Ryan, A. J., in preparation.

(11) Wanka, G.; Hoffmann, H.; Ulbricht, W. *Macromolecules* **1994**, *27*, 4145.

(12) See, for example, Bedells, A. D.; Arafeh, R. M.; Yang, Z.; Attwood, D.; Heatley, F.; Padget, J. C.; Price, C.; Booth, C. *J. Chem. Soc., Faraday Trans.* **1993**, *89*, 1235.

(13) See, for example, Richtering, W. *Prog. Colloid Polym. Sci.* **1997**, *1044*, 90.

(14) Pople, J. A.; Hamley, I. W.; Diakun, G. P. *Rev. Sci. Instrum.* **1998**, *69*, 3015.

(15) Ryan, A. J. *J. Therm. Anal.* **1993**, *40*, 887: Ryan, A. J.; Bras, W.; Mant, G. R.; Derbyshire, G. E. *Polymer* **1994**, *35*, 4537.

(16) Yang, Y.-W.; Ali-Adib, Z.; McKeown, N. B.; Ryan, A. J.; Attwood, D.; Booth, C. *Langmuir* **1997**, *13*, 1860.

(17) Mitchell, D. J.; Tiddy, G. J. T.; Waring, L.; Bostock, T.; McDonald, M. P. M. *J. Chem. Soc., Faraday Trans. 1* **1983**, *79*, 975.

(18) Hvidt, S.; Jørgensen, E. B.; Brown, W.; Schillen, K. *J. Phys. Chem.* **1994**, *98*, 12320.

(19) Jorgensen, E. B.; Hvidt, S.; Brown, W.; Schillen, K. *Macromolecules* **1997**, *30*, 2355.

(20) See, for example, Mortensen, K.; Pedersen, J. S. *Macromolecules* **1993**, *26*, 805; King, S. M.; Heenan, R. K.; Cloke, V. M.; Washington, C. *Macromolecules* **1997**, *30*, 6215.

(21) Pedersen, J. S., private communication, August, 1999.

(22) Lobry, L.; Micali, N.; Mallamace, F.; Liao, C.; Chen, S.-H. *Phys. Rev. E* **1999**, *60*, 7076.

(23) Kelarakis, A.; Havredaki, V.; Derici, L.; Yu, G.-E.; Booth, C.; Hamley, I. W. *J. Chem. Soc., Faraday Trans*. **1998**, *94*, 3639.

(24) Hamley, I. W.; Mortensen, K.; Yu, G.-E.; Booth, C. *Macromolecules* **1998**, *31*, 6958.